

# Effect of electrolytes on the electrochemical behaviour of 11-(ferrocenylcarbonyloxy)undecanethiol SAMs on gold disk electrodes

Huangxian Ju<sup>\*ab</sup> and Dónal Leech<sup>b†</sup>

<sup>a</sup> Department of Chemistry, Nanjing University, Nanjing 210093, China. E-mail: hxju@jlonline.com

<sup>b</sup> Department of Chemistry, University of Montreal, C.P.6128, Succursale A, Montreal, Quebec, Canada H3C 3J7

Received 15th December 1998, Accepted 25th January 1999

The interfacial electrochemistry of mixed monolayers formed by self-assembly from a dilute dodecanethiol-11-(ferrocenylcarbonyloxy)undecanethiol (FcSH) ethanolic solution at pre-treated Au electrodes is reported. The effect of different electrolytes on the interaction among electrochemical products, the interfacial capacitance and the heterogeneous electron transfer rate constant ( $k^0$ ), using fast cyclic voltammetry and chronoamperometry, are examined. The anions have a strong influence on the kinetic and thermodynamic parameters of the interfacial redox reaction through the formation of ion pairs with the oxidized ferrocenium. The ion-pairing capability of various anions with immobilized ferrocenium is compared through evaluation of an effective formation constant. The electrolyte cation is shown to affect the thermodynamics of the ferrocene-ferrocenium electrochemical reaction, with cations of lower mobility shifting the apparent formal potential to more positive potentials, which is explained for the first time with the electric force by means of Debye-Hückel theory. A linear relationship between the apparent formal potential of the ferrocene redox couple in self-assembled monolayers and cation mobility and concentration was observed.

Self-assembled monolayers (SAMs) have received considerable attention recently because of their potential applications in sensing,<sup>1–5</sup> corrosion inhibition and wetting properties<sup>6–9</sup> and in the elucidation of heterogeneous electron transfer mechanisms.<sup>10–20</sup> Most of these reports have focused on alkanethiol monolayers on gold surfaces owing to their ease of preparation and stability.<sup>14–19</sup> The gold topography and surface pre-treatment of the electrodes prior to self-assembly have been shown to affect the quality (defectiveness) of the monolayers produced.<sup>8,21</sup> Mixed monolayers prepared by self-assembly of redox-active ferrocenylalkanethiols and alkanethiols are the most popular surfaces for studies of electron transfer mechanisms.<sup>15–20</sup> Various ratios of redox-active thiol to unsubstituted diluent alkanethiol and self-assembly times have been examined for the production of stable, non-defective, electroactive monolayers.<sup>15,18,19</sup> The effect of the chain length of the alkanethiol on the redox kinetics of the ferrocene-thiol couple in SAMs has been studied.<sup>16,22</sup> The effects of several anions, such as  $\text{ClO}_4^-$ ,  $\text{SO}_4^{2-}$  and  $\text{F}^-$ , on the interfacial formal potential of ferrocenylalkanethiol SAMs have also been reported.<sup>23,24</sup> The effect of anions on the formal potential has been explained by ion pairing between the oxidized ferrocenium cation and the anion. These reports show that the interfacial microstructure and microenvironment of SAMs play an important role in electron transfer processes, but up to now the effect of the cation has not been noted.

Redepenning and Flood<sup>25</sup> described the influence of supporting electrolyte activity on the apparent formal potential and reported that proton and sodium ion activities have little influence on the overall interfacial potential distribution. White *et al.*<sup>26</sup> presented a general theory for the driving force

for reversible electron transfer on SAMs and proposed a special case of the model concerning the influence of the interfacial potential distribution on the voltammetry of electroactive molecular films. These results were based on some simplifying assumptions different from the case of FcSH SAMs. At the FcSH SAMs, the solvent, water molecules and even anions and cations in electrolyte, may permeate into the SAM,<sup>8,27</sup> and the ion-pair formation makes the interfacial potential distribution more complex. Hence it is necessary to investigate the influences of the cation and anion and to search for the internal relationships between the electrochemical behaviours of attached molecules and the stability of SAMs and electrolytes so as to understand in detail the role of the electrolyte in redox processes and rotationally control the interfacial redox behaviour of ferrocenylalkanethiol SAMs.

Here we report on the effects of the anion in the electrolyte on the interaction among cation groups of ferrocenium formed in redox processes and the electrochemistry of an FcSH SAM-modified gold disk electrode. In this work the effect of electrolyte cations is also presented. The results indicate that cations strongly affect the thermodynamics of the ferrocene redox reaction.

## Experimental

### Materials

Gold electrodes were prepared by sealing polycrystalline gold wires (>99.99%) in soft glass tubes using a gas-air flame. The gold electrodes were abraded with successively finer grades of SiC paper and polished to a "mirror-like" finish with 0.3 and 0.05  $\mu\text{m}$  alumina slurry on microcloth pads (Buehler), followed by rinsing with water and ethanol and removal of traces of alumina from the surface by brief cleaning in an ultrasonic

<sup>†</sup> Present address: Department of Chemistry, National University of Ireland, Galway, Ireland.

bath to yield gold disks with macroscopic areas of approximately  $7.0 \times 10^{-3} \text{ cm}^2$ .

All reagents for preparing supporting electrolytes were of reagent grade and were used as received. Electrolyte solutions were prepared in de-ionized water from a Milli-Q purification system. Decanethiol was obtained from Aldrich and used as received. 11-(Ferrocenylcarbonyloxy)undecanethiol was synthesized according to a literature procedure.<sup>15</sup> The product was purified by chromatography on silica gel with methylene chloride and recrystallized from ethanol. Its structure was confirmed by <sup>1</sup>H NMR spectroscopy and elemental analysis. <sup>1</sup>H NMR (500 MHz, CDCl<sub>3</sub>):  $\delta$  1.29 (broad 14H, CH<sub>2</sub>), 1.35 (1H, SH), 1.61 (CH<sub>2</sub>CH<sub>2</sub>SH), 1.72 (2H, CO<sub>2</sub>CH<sub>2</sub>CH<sub>2</sub>), 2.52 (2H, CH<sub>2</sub>SH), 4.20 (5H, C<sub>5</sub>H<sub>5</sub>), 4.21 (2H, CO<sub>2</sub>CH<sub>2</sub>), 4.38 (2H, C<sub>5</sub>H<sub>4</sub>) and 4.80 (2H, C<sub>5</sub>H<sub>5</sub>). Elemental analysis: calculated for C<sub>22</sub>H<sub>32</sub>SO<sub>2</sub>: C, 63.46; H, 7.75; S, 7.70; Fe, 13.41; O, 7.68. Found: C, 63.52; H, 7.54; S, 7.93; Fe, 13.22; O, 7.43%.

### Monolayer formation and electrochemistry

Monolayers were formed by soaking freshly pre-treated electrodes in a coating solution containing various ratios of FcSH to decanethiol with a total concentration of 1.0 mM thiol in absolute ethanol for at least 48 h. With this self-assembly period fewer defect monolayers were obtained.<sup>15</sup>

All electrochemical measurements were performed using a BAS-100B electrochemical analyzer. A conventional three-electrode cell was employed with the SAM-modified electrode as the working electrode, Pt wire as the auxiliary electrode, and Ag/AgCl in 3.0 M NaCl (BAS) as the reference electrode. All potentials are reported *versus* this reference electrode at room temperature (24 °C). Oxygen was not excluded from the cell.

The microscopic area of the unmodified polished gold electrodes was determined by measuring the charge that evolved during oxidation of the superficial gold in 0.1 M H<sub>2</sub>SO<sub>4</sub>.<sup>28</sup> The ratio of microscopic to geometric surface area yielded a roughness factor of  $3.5 \pm 0.5$ .

## Results and discussion

### Choice of pre-treatment method and composition of coating solution

The pre-treatment of polycrystalline gold electrodes prior to self-assembly of thiols has been accomplished by treatment in hot 2 M KOH for 1 h,<sup>14</sup> chemical etching with dilute *aqua regia*,<sup>21</sup> hot piranha solution<sup>1,8</sup> or hot concentrated nitric acid,<sup>22,24</sup> electrochemical etching in dilute H<sub>2</sub>SO<sub>4</sub> by cycling between  $-0.2$  and  $+1.4$  V<sup>29</sup> or by a combination of chemical and electrochemical etching.<sup>11</sup> At the same time, the ratio of diluent alkanethiol to electroactive FcSH in the deposition solution and the self-assembly period are also the important factors for the preparation of ordered self-assembled redox-active monolayers.<sup>15,23</sup> In this work we used a self-assembly period of 48 h (with this period an exchange equilibrium between monolayer and coating solution was reached<sup>15</sup>) to compare different pre-treatment methods and examine the effect of the ratio of FSH to decanethiol in the coating solution on the wave shape and stability of the monolayer in 1.0 M HClO<sub>4</sub>. The results indicated that the FcSH–decanethiol SAMs formed on gold electrodes pre-treated by etching in dilute *aqua regia* gave improved stability and responses with a small peak potential splitting ( $<28$  mV for the coating solution with an FcSH to decanethiol ratio of 0.5 : 0.5) at scan rates less than  $10 \text{ V s}^{-1}$ . Thus, the kinetics of the heterogeneous electron transfer reaction to and from the ferrocene moiety, qualitatively observed from the peak potential splitting of the CVs, is rapid. Furthermore, the cell resistance is very low at an electrolyte concentration of 1.0 M ( $<100 \Omega$  determined at rest potential). The cyclic voltammograms (not

shown) of the SAMs produced from 0.1 : 0.9, 0.5 : 0.5 and 0.9 : 0.9 FcSH–decanethiol coating solutions at the same scan rate displayed different peak shapes and potential separations. The SAMs obtained by adsorption from 0.5 : 0.5 FcSH–decanethiol solution yielded the most “ideal” electrochemical responses. We therefore selected the *aqua regia* pre-treatment and this ratio to prepare the SAMs for all subsequent studies. In these SAMs the average coverage of ferrocene units is  $(1.3 \pm 0.3) \times 10^{-10} \text{ mol cm}^{-2}$ , calculated from the peak area of the cyclic voltammograms at  $1 \text{ V s}^{-1}$ .

### Influence of electrolyte on interaction parameters and capacitance

Fig. 1 shows the cyclic voltammograms of a SAM in 1.0 M HClO<sub>4</sub>. A symmetric waveshape with a small peak-to-peak potential separation ( $\Delta E_p < 20$  mV for scan rates  $<1 \text{ V s}^{-1}$ ) was obtained for the ferrocene/ferrocenium (Fc<sup>0</sup>/Fc<sup>+</sup>) redox couple within the SAM. The shape of the voltammogram and  $\Delta E_p$  were independent of scan rate ( $v$ ) for scan rates less than  $1 \text{ V s}^{-1}$ , and the peak currents increased linearly with increasing scan rate, as expected for a rapid reversible electrode process to an immobilized redox couple. Both peak potential splitting and its change were also very small in the scan rate range  $1$ – $10 \text{ V s}^{-1}$ . When the scan rate was more than  $10 \text{ V s}^{-1}$ , the splitting obviously increased with increasing scan rate. These behaviours are similar to the model of Brown and Anson.<sup>30</sup> According to Brown and Anson, the small peak potential separation at low scan rate can be interpreted in terms of an interaction parameter. The interaction parameter describes the perturbing influence experienced by a given molecule of attached oxidant or reductant due to the presence of the other attached oxidant and reductant molecules. The interaction parameter equation is expressed as<sup>30</sup>

$$i_p = \frac{n^2 F^2 A \Gamma v}{RT[4 - \Gamma(\gamma_O + \gamma_R)]} \quad (1)$$

where  $\gamma_O$  and  $\gamma_R$  are the non-ideality parameters of attached oxidant and reductant, respectively, which result from the interaction between attached molecules, and the other parameters have their usual meanings. At scan rates less than  $1 \text{ V s}^{-1}$ , the slopes of plots of peak current *versus*  $v$  in various electrolytes of HClO<sub>4</sub>, LiClO<sub>4</sub>, NaClO<sub>4</sub>, NaBF<sub>4</sub>, NaNO<sub>3</sub> and Na<sub>2</sub>SO<sub>4</sub> were 1.00, 1.04, 1.06, 0.83, 0.45 and  $0.19 \mu\text{A s V}^{-1}$ , respectively, yielding the  $(\gamma_O + \gamma_R)$  of  $-(6.1, 5.8, 5.6, 8.1, 17$  and

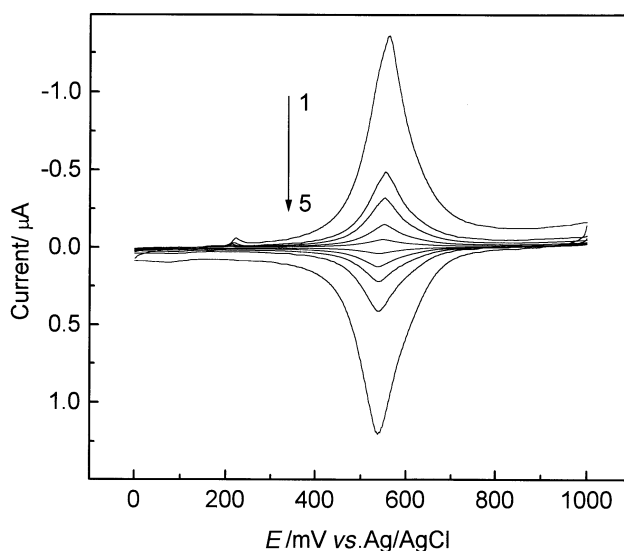


Fig. 1 Cyclic voltammograms of FcSH SAM [ $\Gamma = (1.4 \pm 0.5) \times 10^{-10} \text{ mol cm}^{-2}$ ] at (1) 300, (2) 100, (3) 60, (4) 30 and (5)  $10 \text{ mV s}^{-1}$  in 1.0 M HClO<sub>4</sub>.

**Table 1** Redox and ion-pairing properties of the FcSH monolayers (prepared according to the text) in various electrolyte solutions

Electrolyte (1.0 M)	$E_{\text{SAM}}^{\circ}/\text{mV}$	$C_{\text{m}}^d/\mu\text{F cm}^{-2}$	$k^0e/\text{s}^{-1}$	$K_{\text{X}^-}/K_{\text{Cl}^-}$ <sup>f</sup>	$K_{\text{eff}}^g/\text{M}^{-1}$
HClO <sub>4</sub>	520	1.1 ± 0.5	648 ± 29	—	—
NaClO <sub>4</sub>	576	1.7 ± 0.5	654 ± 23	47.5	1785
NaBF <sub>4</sub> <sup>a</sup>	606	1.8 ± 0.8	551 ± 22	42.0	413
NaNO <sub>3</sub>	630	2.8 ± 1.0	510 ± 26	5.8	77
NaCl	675	3.0 ± 0.4	482 ± 26	1.0	—
Na <sub>2</sub> SO <sub>4</sub>	700	2.0 ± 0.5	488 ± 25	1.2	8
CH <sub>3</sub> COONa	680	3.1 ± 0.1	—	0.8	—
NaF	684	3.4 ± 0.5	—	0.7	—
PB <sup>b</sup>	674	2.9 ± 0.6	—	1.0	—

<sup>a</sup> Concentration 0.35 M. <sup>b</sup> Phosphate buffer (pH 7.2), prepared from 1.0 M solutions of Na<sub>2</sub>HPO<sub>4</sub> and NaH<sub>2</sub>PO<sub>4</sub> salts. <sup>c</sup> Evaluated from the average CV peak potentials at 10 V s<sup>-1</sup>. <sup>d</sup> Evaluated from CV currents approximately 400 mV negative of  $E_{\text{SAM}}^{\circ}$ . <sup>e</sup> Evaluated from the intercept of the anodic portion of a Tafel plot, constructed from results obtained by chronoamperometry at various overpotentials [eqn. (2)]. <sup>f</sup> Relative ion-pairing ability of electrolyte anions with respect to that of a separate solution of containing chloride anions [eqn. (6)]. <sup>g</sup> Effective ion-pair formation constants for the electrolyte anions determined from mixed solutions of the anion in 1.0 M NaCl [eqn. (7)].

$46) \times 10^{10} \text{ cm}^2 \text{ mol}^{-1}$ , respectively. Negative values for all interaction parameters are an indication that the process responsible for the non-ideality is a repulsion between attached reactants. Similar ( $\gamma_{\text{O}} + \gamma_{\text{R}}$ ) values obtained in HClO<sub>4</sub>, LiClO<sub>4</sub> and NaClO<sub>4</sub> electrolytes indicate little effect of cations on the response. Larger negative values of interaction parameters are obtained in electrolytes containing anions that do not strongly ion-pair with the oxidized ferrocenium ion (see below). The stabilizing nature of the strong ion pair on the oxidized form of ferrocene thus decreases the non-ideal interactions between adjacent redox active molecules adsorbed on the surface.

Measurement of interfacial capacitance has frequently been used to verify the quality of packing of SAMs.<sup>12,31</sup> For FcSH SAMs, ions and solvent can permeate the monolayer depending on the length of the diluent alkanethiol.<sup>13,21</sup> Ion permeation through the monolayer results in a dependence of capacitance on the electrolyte. In this work, capacitance was evaluated from the cyclic voltammetric charging currents at rest potential (determined under open circuit, typically between 0 and 100 mV), far from the ferrocene formal potential. For a SAM electrode the double layer structure may be considered as an ideal compact monolayer capacitor ( $C_{\text{m}}$ ) and a diffuse double layer capacitor ( $C_{\text{dl}}$ ) connected in series.<sup>31</sup>  $C_{\text{dl}}$  can be estimated from Gouy–Chapman theory,<sup>32</sup> and is much larger than the monolayer capacitance and can therefore be neglected.<sup>31</sup> Therefore

$$C_{\text{total}} \approx C_{\text{m}} = \frac{\epsilon\epsilon_0}{d} \quad (2)$$

where  $\epsilon$  is the dielectric constant of the monolayer,  $\epsilon_0 = 8.85 \times 10^{-14} \text{ F cm}^{-1}$  and  $d$  is the monolayer thickness [2.5 nm for FcCOO(CH<sub>2</sub>)<sub>11</sub>SH and 1.7 nm for decanethiol].<sup>15</sup> The results of capacitance measurements are summarized in Table 1. The capacitance is dependent on both cation and anion in solution. In HClO<sub>4</sub>  $\epsilon = 3.24$ , which is close to the literature value of 3.<sup>12</sup> The value in NaClO<sub>4</sub> is 4.96, which is larger than that in HClO<sub>4</sub> owing to the smaller cationic radius of the sodium ion. The smaller the effective cationic radius, the higher is the capacitance because more cations permeate into the SAM, increasing the dielectric constant. A lower SAM capacitance in ClO<sub>4</sub><sup>-</sup> solution compared with other anions indicates that ClO<sub>4</sub><sup>-</sup> causes the monolayer to be much more

compact, containing less solvent and being less permeable to the supporting electrolyte.

### Electron transfer kinetics in various electrolytes

The standard heterogeneous electron transfer rate constant,  $k^0$ , for irreversibly adsorbed redox-active molecules can be conveniently evaluated from chronoamperometric experiments if the RC cell time constant is sufficiently short. In this work the electrode potential was stepped from an initial potential (rest potentials of the SAM in various electrolytes) to a final potential to drive the oxidation of ferrocene groups. At a given overpotential ( $\eta = E - E_{\text{SAM}}^{\circ}$ , where  $E_{\text{SAM}}^{\circ}$  is the formal potential estimated from the mean of the anodic and cathodic peak potentials in slow-scan cyclic voltammetry), the Faradaic current  $I$  follows a simple exponential decay given by<sup>20</sup>

$$I(t) = k_{\text{app}} Q \exp(-k_{\text{app}} t) \quad (3)$$

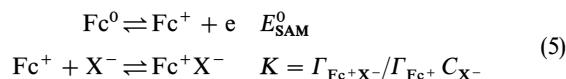
where  $k_{\text{app}}$  is the apparent rate constant and  $Q$  is the electrolytic charge passed. From the slope of a plot of  $\ln i$  versus  $t$  at electrolysis times of 0.5–3.5 ms [here the RC cell time constants are typically less than 0.03 ms and the effect of ohmic drop (<2 mV) can be neglected], average rate constants at different overpotentials in various electrolytes can be estimated. The  $k^0$  values can be evaluated from the intercept of a semilogarithmic plot (Tafel plot) of  $k_{\text{app}}$  versus overpotential,  $\eta$ , according to the Butler–Volmer formalism described by the equation<sup>32</sup>

$$k_{\text{app}} = k^0 \exp[(1 - \alpha)nF\eta/RT] \quad (4)$$

The values of  $k^0$  for SAMs together with their formal potentials in various electrolytes are listed in Table 1. A  $k^0$  value of 648 s<sup>-1</sup> evaluated from the anodic intercept of the Tafel plot in 1 M HClO<sub>4</sub> is similar to the value of 665 s<sup>-1</sup> estimated by extrapolation of data (Fig. 11 in ref. 16) obtained by an indirect laser induced temperature jump method. The values of  $k^0$  obtained in HClO<sub>4</sub> and NaClO<sub>4</sub> electrolyte are extremely close. The value of  $k^0$  seems to be dependent on the electrolyte anion, with a maximum decrease of 26% obtained in NaCl electrolyte compared with that for the perchlorate electrolytes. However, the instability of the FcSH monolayers in chloride electrolyte should be noted.<sup>9</sup> The observed decrease in  $k^0$  in the chloride or sulfate electrolyte may be attributed to a gradual decrease in their ion-pairing ability with the ferrocenium cation. In any event, the relatively rapid rates of heterogeneous electron transfer at these SAMs allow us to use the Nernst equation to evaluate ion-pair formation in various electrolytes at scan rates where the surface reaction yields reversible behaviour.

### Ion-pair formation

In the cyclic voltammetric experiments, the formal redox potential of the ferrocene groups in the monolayer shifts negatively with increasing anion concentration. This phenomenon has been reported previously.<sup>23,25,27,29</sup> The effect can be explained by the need to neutralize the excess charge that builds up at the interface upon oxidation and to stabilize the ferrocenium ion in the non-polar environment of the assembled monolayers.<sup>29</sup> The formation of a 1 : 1 ion pair can be expressed as



According to the Nernst equation, the potential for the above half-reaction can be written as follows:

$$E_{\text{SAM}}^{\circ} = E_{\text{SAM}}^{\circ} + \frac{RT}{F} \log \frac{\Gamma_{\text{Fc}^+\text{X}^-}}{\Gamma_{\text{Fc}^{\circ}} K} - \frac{RT}{F} \log C_{\text{X}^-} \quad (6)$$

Hence there is a quantitative relationship between the ion-pairing ability (formation constant  $K$ ) and the formal potential,  $E_{\text{SAM}}^{0'}$ . The linear relationship observed between  $E_{\text{SAM}}^{0'}$  and the logarithm of the  $\text{ClO}_4^-$  concentration in  $\text{NaClO}_4$  electrolyte is shown in Fig. 2. The slope of  $-65$  mV, close to the Nernstian value of  $-59$  mV predicted from eqn. (6), agrees with the hypothesis that there is the formation of a single ion pair with the ferrocenium in the SAMs. A negligible difference in the slope is obtained if activities are used instead of concentrations (slope of  $-67$  mV).

Ion-pairing tendencies of various anions with the ferrocenium cation could be quantitatively compared using eqn. (6) if the standard potential of ferrocene in the SAM was available. We can compare the relative ion-pairing ability between solutions of individual electrolytes by use of eqn. (7) and selecting the chloride anion as reference.

$$\frac{K_{\text{X}^-}}{K_{\text{Cl}^-}} = \frac{C_{\text{Cl}^-}}{C_{\text{X}^-}} \exp\left[\frac{F(E_{\text{Cl}^-}^{0'} - E_{\text{X}^-}^{0'})}{RT}\right] \quad (7)$$

The results shown in Table 1 (we neglected the formation of  $\text{Fc}_2^+\text{SO}_4^{2-}$  for  $\text{Na}_2\text{SO}_4$  as a supporting electrolyte) indicate that  $\text{BF}_4^-$  forms almost as strong an ion pair as  $\text{ClO}_4^-$  with the ferrocenium cation. The  $\text{ClO}_4^-$  and  $\text{BF}_4^-$  anions can be transported with almost no associated solvent, water, and are thus hydrophobic anions which ion-pair strongly to ferrocenium.  $\text{NO}_3^-$ ,  $\text{Cl}^-$ ,  $\text{SO}_4^{2-}$ ,  $\text{HPO}_4^{2-}$ ,  $\text{H}_2\text{PO}_4^-$ , and particularly  $\text{F}^-$ , more hydrophilic anions, are transported with large amounts of solvent,<sup>27</sup> and thus may interact less with the ferrocenium cation. In the  $\text{ClO}_4^-$  and  $\text{BF}_4^-$  electrolytes no loss of ferrocene adsorbate is apparent upon repeated cycling for long times, demonstrating the high stability imparted by ion-pair formation between the desolvated anions and the oxidized FcSH monolayers. The ferrocene redox peak currents decrease slightly upon continuous cycling in the  $\text{NaNO}_3$ ,  $\text{Na}_2\text{SO}_4$ ,  $\text{NaCl}$  electrolytes and disappear rapidly in  $\text{CH}_3\text{COONa}$ ,  $\text{Na}$  phosphate and  $\text{NaF}$  electrolytes. Hence the formation of ion pairs greatly improves the stability of FcSH SAMs.

To investigate this phenomenon further we performed experiments in which the ionic strength of the electrolyte was maintained high, with a background electrolyte of  $1.0$  M  $\text{NaCl}$ , during the addition of  $\text{NaClO}_4$ , to avoid liquid junction and activity effects. A chloride electrolyte was selected because of its low ion-pairing ability compared with other anions. A semilogarithmic plot is shown in Fig. 3, giving a slope of  $-59$

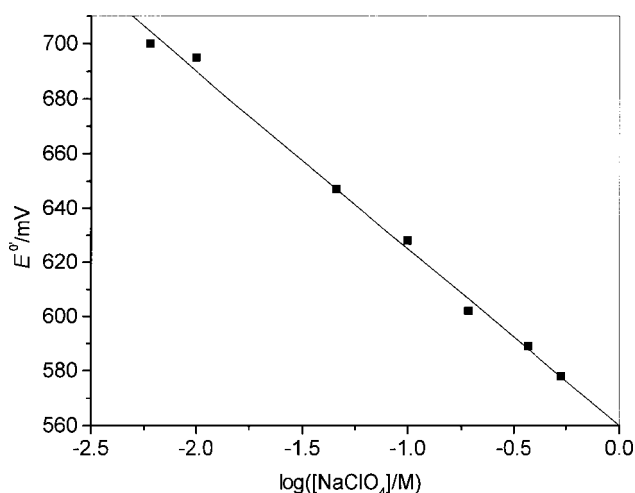


Fig. 2 Dependence of the formal potential of FcSH SAM, from cyclic voltammograms at  $10$  V  $\text{s}^{-1}$ , on sodium perchlorate electrolyte concentration.  $\Gamma = (1.2 \pm 0.2) \times 10^{-10}$  mol  $\text{cm}^{-2}$ .

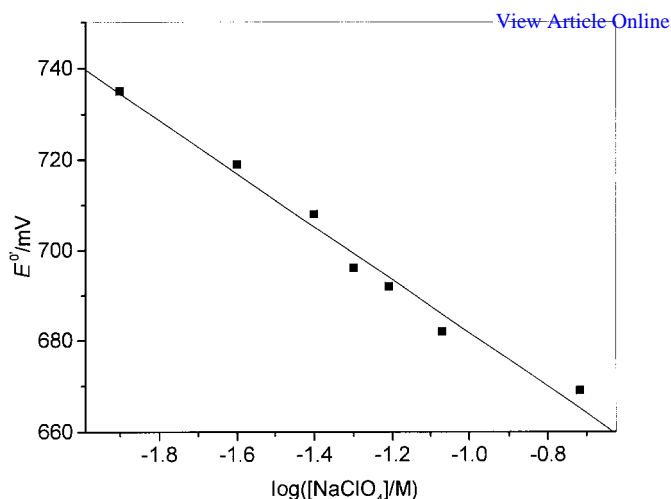


Fig. 3 Dependence of the formal potential of FcSH SAM on sodium perchlorate concentration in solutions containing  $1.0$  M  $\text{NaCl}$  as background electrolyte. Other conditions as in Fig. 2.

mV as expected for ion pairing of the ferrocenium cation by a single perchlorate anion upon oxidation of the SAM.

Rowe and Creager<sup>23</sup> have described the ion-pairing ability of anions  $\text{Y}^-$  in the presence of excess  $\text{X}^-$  electrolyte anions with an effective formation constant,  $K_{\text{eff}}$ , evaluated using the following equation:

$$E_p = E_p' - (RT/nF)\ln(1 + K_{\text{eff}} C_y) \quad (8)$$

where  $E_p$  and  $E_p'$  are the anodic peak potentials in electrolytes with and without anion  $\text{Y}^-$  present, respectively, and  $K_{\text{eff}} = K_y/(1 + K_x C_y)$ . If the assumption is made that the predominant ion-pairing anion is  $\text{Y}^-$ , then  $K_{\text{eff}} C_y \gg 1$  and eqn. (8) becomes

$$E_p = E_p' - (RT/nF)\ln(K_{\text{eff}} C_y) \quad (9)$$

Effective ion-pair formation constants were determined for the sodium salts of the  $\text{ClO}_4^-$ ,  $\text{BF}_4^-$  and  $\text{NO}_3^-$  anions in  $\text{NaCl}$  solutions and the results are given in Table 1. The sequence of  $K_{\text{eff}}$  for various anions is similar to that of the ratios observed in individual solutions and again reflects the dependence of the solvation and hydrophilicity of the various anions on their ion-pairing ability with the ferrocenium cation.

Comparing ion-pairing ability with the peak separation and wave shape of cyclic voltammograms, the interaction parameters, the capacitance, the stability and the electron transfer kinetics, it can be found that all parameters show the same tendency for change, which is identical with the change in ion-pairing ability.

### Electrolyte cation effects

In the electrochemical process, the ferrocenium cation formed upon oxidation of the FcSH monolayer will establish an electric field that repels the electrolyte cations and attracts the electrolyte anions. According to the Debye-Hückel theory,<sup>33,34</sup> in a solution of low concentration electrolytes the work done during ion transport of cations from the monolayer surface to the bulk solution upon oxidation is the change in the Gibbs energy,  $\Delta G_{\text{electric}}$ , given by

$$\Delta G_{\text{electric}} = \pm \sum_j \frac{N_j z_j e^2 K}{3\epsilon} \quad (10)$$

where  $j$  is the kind of ion in solution,  $N_j$  is the total number of ion  $j$ ,  $e$  is the elementary charge,  $z$  is the charge of ion  $j$ ,  $\epsilon$  is the dielectric constant of the medium and  $1/K$  is the Debye-Hückel reciprocal length representing the effective radius of

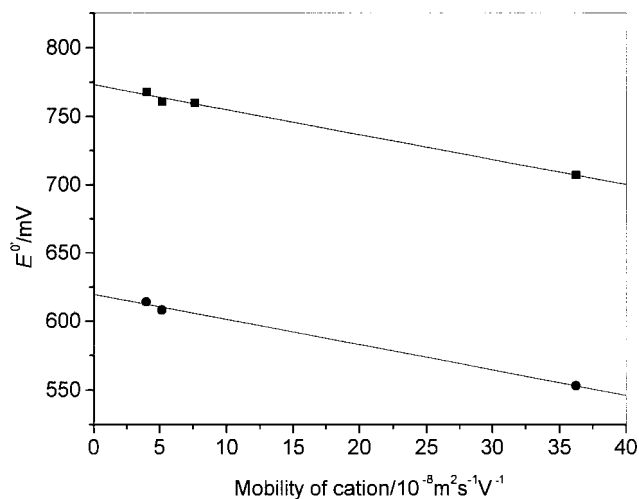


**Fig. 4** Dependence of the formal potential of FcSH SAM, evaluated from cyclic voltammograms in 1.0 M perchlorate (●) or chloride (■) electrolytes, on the cation mobility. The cations are  $\text{Li}^+$ ,  $\text{Na}^+$ ,  $\text{K}^+$  and  $\text{H}^+$  from left to right, respectively.  $\Gamma = (1.5 \pm 0.3) \times 10^{-10} \text{ mol cm}^{-2}$ ; other conditions as in Fig. 2.

the ionic atmosphere around a given ion in an electrolyte solution. In aqueous solution  $a$  is the effective radius of ion, taking into account all the  $\text{H}_2\text{O}$  molecules which the ion carries in its hydration sphere (hydrodynamic radius). The relationship between the ion radius  $a$  and the ionic mobility,  $\mu$ , is given by<sup>35</sup>

$$\mu = ze/6\pi\eta a \quad (11)$$

where  $\eta$  is the viscosity of the medium. The radius of the ionic atmosphere surrounding an ion is related to both its charge and its hydrodynamic radius. If one makes a simplistic assumption, replacing  $K$  with  $\xi/a$  for qualitatively associating  $\Delta G_{\text{electric}}$  with the mobility (where  $\xi$  depends on the ionic charge, temperature, dielectric constant and ionic strength of the medium), then eqn. (10) becomes

$$\Delta G_{\text{electric}} = \pm \sum_j \frac{2\pi\xi N_j \eta \mu_j e}{\epsilon} \quad (12)$$

Hence transport of cations from the monolayer to the bulk solution upon oxidation of the attached ferrocene to ferrocenium requires free energy of transfer. Considering the dif-

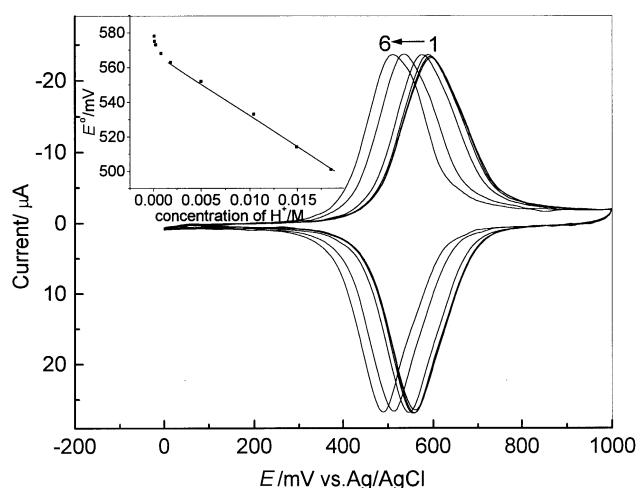


**Fig. 5** Cyclic voltammograms of a FcSH SAM in 1.0 M  $\text{NaClO}_4$  at  $10 \text{ V s}^{-1}$  on addition of (1) 0, (2) 0.001, (3) 0.011, (4) 0.115, (5) 0.604 and (6) 1.06 M  $\text{HClO}_4$  to the cell. Inset: plot of formal potential versus proton concentration.  $\Gamma = (1.2 \pm 0.2) \times 10^{-10} \text{ mol cm}^{-2}$ .

ference between thermodynamic and transport parameters, a correction factor,  $\zeta$ , is given for qualitatively associating the change in the Gibbs energy with the additional potential,  $\Delta E$ , and then

$$\Delta E = \mp \sum_j \frac{2\pi\xi\zeta N_j \eta \mu_j e}{nF\epsilon} \quad (13)$$

If other conditions are constant, an additional potential is necessary to drive this transport. The negative additional potential indicates the repulsion between monolayer ferrocenium cation and electrolyte cations. Hence there is a linear relationship with a negative slope value between apparent formal potential and cation mobility or concentration ( $N$ ).

In order to rectify the formal potentials obtained, the liquid junction potentials,  $E_j$ , in these systems were determined by using two  $\text{Ag}/\text{AgCl}$  (3 M  $\text{NaCl}$ ) reference electrodes to create two half cells which were contacted by a salt bridge of 3 M  $\text{KCl}$  in agar. 3 M  $\text{NaCl}$  and the above solutions were used in the two half cells as the electrolytes. The results showed that the  $E_j$  between 3 M  $\text{NaCl}$  and 1 M  $\text{LiClO}_4$ ,  $\text{NaClO}_4$ ,  $\text{HClO}_4$ ,  $\text{LiCl}$ ,  $\text{NaCl}$ ,  $\text{KCl}$  or  $\text{HCl}$  was 2.1, 2.3, 3.7, 2.0, 2.2, 2.5 or 3.5 mV, respectively. All these values and the differences among them were very small because high concentration electrolytes were used in our experiments, as in those reported in the literature.<sup>36</sup>

The experimental relationship between formal potentials of FcSH monolayers and cation mobility<sup>35</sup> in both perchlorate and chloride electrolytes is shown in Fig. 4. A linear relationship with a correlation coefficient of 0.9991 between two parameters for these monolayers is obtained. The slope of line is the same in 1.0 M electrolytes of both perchlorate and chloride anions, so supporting quantitatively eqn. (13).

In perchlorate electrolyte the formal potential also shifts in proportion to the proton concentration ( $N_{\text{H}^+}$ ), as can be seen in Fig. 5. Although the concentration of the  $\text{ClO}_4^-$  anion changes only from 1.0 to 1.02 M (calculated from the acid dissociation constant of  $1.78 \times 10^{-2} \text{ M}$  for  $\text{HClO}_4$ <sup>35</sup>), the FcSH formal potential shifts negatively by approximately 77 mV. Furthermore, there is a linear relationship between the FcSH formal potential and proton concentration from 0.0018 to 0.018 M with a correlation coefficient of 0.9994 (inset in Fig. 5). It is conceivable that when the electrolyte solution includes several cations, the migration of cations during oxidation is mainly undertaken by those cations with high mobilities once present in sufficiently high concentrations. These two effects confirm that eqn. (13) represents a simplistic qualitative model of the system.

## Conclusion

We have found that stable and well behaved redox-active monolayers can be prepared on gold disk electrodes pre-treated with dilute *aqua regia* from a mixed ethanolic solution of 0.5 mM FcSH–0.5 mM decanethiol. The electrolyte anions have a strong effect on the thermodynamics of the ferrocene interfacial redox reaction. This effect can be modelled on their relative abilities to form ion pairs with the oxidized ferrocenium ion. The effective ion-pair formation constant for various anions are reported, with perchlorate yielding the largest value. The electrolyte type affects the interactions between the ferrocene redox species in the monolayer, the interfacial capacitance, the stability of SAMs and the heterogeneous electron transfer rate constants, and their tendency for change is identical with the change in ion-pairing ability. The electrolyte cations are also shown to affect the thermodynamics of the ferrocene redox reaction, postulated to be due to electrostatic effects upon oxidation of the ferrocene to a ferrocenium form. The results presented yield information on the optimum conditions for producing and maintaining stable,

reproducible electroactive monolayers and provide a basis for future studies on their application as sensing materials.

This work was supported by the University of Montreal and the Natural Sciences and Engineering Research Council of Canada. H.J. acknowledges financial support from the Ministry of Education of China.

## References

- 1 S. Rubin, J. T. Chow, J. P. Ferraris and T. A. Zawodzinski, Jr., *Langmuir*, 1996, **12**, 363.
- 2 I. Rubinstein, S. Steinberg, Y. Tor, A. Shanzer and J. Sagiv, *Nature (London)*, 1988, **332**, 426.
- 3 J. J. Hickman, D. Ofer, P. E. Laibinis, G. M. Whitesides and M. Wrighton, *Science*, 1991, **252**, 688.
- 4 K. Uosaki, Y. Sato and H. Kita, *Electrochim. Acta*, 1991, **36**, 1799.
- 5 L. J. Kepley, R. M. Crooks and A. J. Ricco, *Anal. Chem.*, 1992, **64**, 3191.
- 6 O. Chailapakul, L. Sun, C. Xu and R. M. Crooks, *J. Am. Chem. Soc.*, 1993, **115**, 12459.
- 7 R. G. Nuzzo and D. L. Allara, *J. Am. Chem. Soc.*, 1983, **105**, 4481.
- 8 M. D. Porter, T. B. Bright, D. L. Allara and C. E. D. Chidsey, *J. Am. Chem. Soc.*, 1987, **109**, 3559.
- 9 N. L. Abbott and G. M. Whitesides, *Langmuir*, 1994, **10**, 1493.
- 10 E. Sabatani and I. Rubinstein, *J. Phys. Chem.*, 1987, **91**, 6663.
- 11 H. O. Finklea and D. D. Hanshew, *J. Am. Chem. Soc.*, 1992, **114**, 3173.
- 12 C. Miller, P. Cuendet and M. Grätzel, *J. Phys. Chem.*, 1991, **95**, 877.
- 13 A. M. Becka and C. J. Miller, *J. Phys. Chem.*, 1993, **97**, 6233.
- 14 E. Katz, N. Itzhak and I. Willner, *Langmuir*, 1993, **9**, 1392.
- 15 C. E. D. Chidsey, C. R. Bertozzi, T. M. Putvinski and A. M. Mujisce, *J. Am. Chem. Soc.*, 1990, **112**, 4301.
- 16 J. F. Smally, S. W. Feldberg, C. E. D. Chidsey, M. R. Linford, M. D. Dewton and Y. P. Liu, *J. Phys. Chem.*, 1995, **99**, 13141.
- 17 J. N. Richardson, G. K. Rowe, M. T. Carter, L. M. Tender, L. S. Curtin, S. R. Peck and R. W. Murray, *Electrochim. Acta*, 1995, **40**, 1331.
- 18 S. E. Creager and G. K. Rowe, *Langmuir*, 1994, **10**, 1186.
- 19 D. M. Collard and M. A. Fox, *Langmuir*, 1991, **7**, 1192.
- 20 R. J. Forster and L. R. Faulker, *J. Am. Chem. Soc.*, 1994, **116**, 5444 and 5453.
- 21 S. E. Creager, L. A. Hockett and G. K. Rowe, *Langmuir*, 1992, **8**, 854.
- 22 L. H. Guo, J. S. Facci and G. McLendon, *J. Phys. Chem.*, 1995, **99**, 8458.
- 23 G. K. Rowe and S. E. Creager, *Langmuir*, 1991, **7**, 2307.
- 24 S. E. Creager and G. K. Rowe, *Anal. Chim. Acta*, 1991, **246**, 233.
- 25 J. Redepenning and J. M. Flood, *Langmuir*, 1996, **12**, 508.
- 26 C. P. Smith and H. S. White, *Anal. Chem.*, 1992, **64**, 2398; *Langmuir*, 1993, **9**, 1; X. Gao, H. S. White, S. Chen and H. D. Abruna, 1995, **11**, 4554.
- 27 H. C. De Long and D. A. Buttry, *Langmuir*, 1990, **6**, 1319.
- 28 U. Oesch and J. Janata, *Electrochim. Acta*, 1983, **28**, 1237.
- 29 M. T. Cruanes, H. G. Drickamer and L. R. Faulkner, *Langmuir*, 1995, **11**, 4089.
- 30 A. P. Brown and F. C. Anson, *Anal. Chem.*, 1977, **49**, 1589.
- 31 Q. Cheng and A. Brajter-Toth, *Anal. Chem.*, 1995, **67**, 2767.
- 32 A. J. Bard and L. R. Faulkner, *Electrochemical Methods: Fundamentals and Applications*, Wiley, New York, 1980, p. 91–92 and 500–511.
- 33 P. Debye and E. Hückel, *Z. Phys.*, 1923, **24**, 305.
- 34 S. Petrucci, *Ionic Interactions: Vol I. Equilibrium and Mass Transport*, Academic Press, New York, 1971, p. 5–16.
- 35 P. Atkins, *Physical Chemistry*, Freeman, San Francisco, 5th edn., 1994, pp. 839–841 and C28.
- 36 J. Redepenning, H. M. Tunison and H. O. Finklea, *Langmuir*, 1993, **9**, 1404.

Paper 8/09754B